The NC1/Endostatin Domain of *Caenorhabditis elegans* Type XVIII Collagen Affects Cell Migration and Axon Guidance

Brian D. Ackley,* Jennifer R. Crew,* Harri Elamaa,‡ Tania Pihlajaniemi,‡ Calvin J. Kuo,§ and James M. Kramer*

*Department of Cell and Molecular Biology, Northwestern University Medical School, Chicago, Illinois 60611; ‡Collagen Research Unit, Biocenter, and Department of Medical Biochemistry, University of Oulu, FIN-90014 Oulu, Finland; and §Department of Surgery, Children's Hospital, Harvard Medical School, Boston, Massachusetts 02115

Abstract. Type XVIII collagen is a homotrimeric basement membrane molecule of unknown function, whose COOH-terminal NC1 domain contains endostatin (ES), a potent antiangiogenic agent. The *Caenorhabditis elegans* collagen XVIII homologue, *cle-1*, encodes three developmentally regulated protein isoforms expressed predominantly in neurons. The CLE-1 protein is found in low amounts in all basement membranes but accumulates at high levels in the nervous system. Deletion of the *cle-1* NC1 domain results in viable fertile animals that display multiple cell migration and axon guidance defects. Particular defects can be rescued by ectopic expression of the NC1 domain, which is shown to be capable of forming trimers. In contrast, expression of monomeric ES does not rescue but dominantly causes cell and axon migration defects that phenocopy the NC1 deletion, suggesting that ES inhibits the promigratory activity of the NC1 domain. These results indicate that the *cle-1* NC1/ES domain regulates cell and axon migrations in *C. elegans.*

Key words: cell migration • neurogenesis • endostatin • collagen • *Caenorhabditis elegans*

Introduction

Basement membranes are specialized zones of extracellular matrix (ECM)[1] that perform essential mechanical and signaling roles in development. Besides providing structural support, the ECM modulates the complex array of signals presented to cells during development and normal homeostasis. Components of the ECM—for example, netrin (Culotti and Merz, 1998)—signal to cells directly, whereas others localize latent growth factor signaling molecules and/or act as cofactors in growth factor signaling (Dinbergs et al., 1996). In addition, basement membrane degradation produces proteolytic fragments that can reveal cryptic ligands that affect cellular processes (Stringa et al., 2000). The best characterized cell–ECM interactions are mediated through integrins (Jones and Walker, 1999), but additional matrix receptors have been identified, such as dystroglycan (Hemler, 1999) and discoidin domain receptors (Vogel, 1999).

Genetic characterization of basement membrane components and their receptors in *Caenorhabditis elegans* has been used to understand the in vivo functions for some of these molecules. Mutations in genes encoding type IV collagen chains *emb-9* and *let-2* (Guo et al., 1991; Sibley et al., 1994), perlecan *unc-52* (Rogalski et al., 1993), alpha integrins *ina-1* (Baum and Garriga, 1997) and *pat-2* (Williams and Waterston, 1994), and beta integrin *pat-3* (Gettner et al., 1995) can result in lethality. Mutations in other *C. elegans* basement membrane components are nonlethal but do affect developmental functions, such as neurogenesis. The null phenotypes for the genes encoding nidogen *nid-1* (Kang and Kramer, 2000; Kim and Wadsworth, 2000) and netrin *unc-6* (Ishii et al., 1992) are cell migration and axon guidance defects in the nervous system. In addition, mutations that abrogate the function of specific domains of INA-1 result in cell migration defects (Baum and Garriga, 1997). It is apparent that ECM molecules or their subdomains can provide distinct signaling and structural functions.

Vertebrate type XV and XVIII collagens are closely related basement membrane molecules of unknown function (Kivirikko et al., 1994; Muragaki et al., 1994; Oh et al., 1994a; Rehn et al., 1994). Both collagens are broadly expressed and have been localized to a wide variety of basement membranes, including those of the endothe-

Address correspondence to James M. Kramer, Department of Cell and Molecular Biology, Northwestern University Medical School, 303 East Chicago Ave., Chicago, IL 60611. Tel.: (312) 503-7644. Fax: (312) 503-7912. E-mail: jkramer@nwu.edu

[1]*Abbreviations used in this paper:* dsRNA, double-stranded RNA; ECM, extracellular matrix; EGS, ethylene glycol bis-succinic acid; ES, endostatin; GFP, green fluorescent protein; HSN, hermaphrodite-specific neuron; RNAi, RNA interference; RT, reverse transcription.

Published March 19, 2001

lium, epidermis, kidney, lung, liver, peripheral nerves, and brain (Oh et al., 1994b; Rehn and Pihlajaniemi, 1994, 1995; Muragaki et al., 1995; Hagg et al., 1997; Musso et al., 1998; Saarela et al., 1998a,b; Sasaki et al., 1998). The COOH-terminal 20-kD fragment of type XVIII collagen, termed endostatin (ES), was isolated from tumor cell culture medium as an inhibitor of endothelial cell proliferation. ES has been shown to inhibit endothelial cell proliferation and migration and angiogenesis both in vivo and in vitro (O'Reilly et al., 1997; Yamaguchi et al., 1999). ES has also been reported to induce apoptosis of appropriately stimulated endothelial cells in vitro (Dhanabal et al., 1999). Treatment of mice bearing experimental tumors with ES can result in tumor regression and dormancy (Boehm et al., 1997; O'Reilly et al., 1997). The equivalent COOH-terminal fragment of type XV collagen, termed restin, has also been reported to inhibit angiogenesis and endothelial cell migration (Ramchandran et al., 1999).

The complete 38-kD COOH-terminal noncollagenous domain of type XVIII collagen, termed NC1, has been identified in tissue homogenates, suggesting that it exists as a physiologic cleavage product (Sasaki et al., 1998). At least three functional elements exist within the NC1 fragment: an association domain, a proteolytically sensitive hinge region, and the ES domain. NC1 domains oligomerize noncovalently into trimers through their association domain, whereas ES remains monomeric. NC1 oligomers also show a pattern of interactions with other matrix molecules that is distinct from ES, indicating that the NC1 and ES fragments of type XVIII collagen may have distinct functions (Sasaki et al., 1998, 2000).

We have identified a type XV/XVIII collagen homologue in *C. elegans*, designated *cle-1*. We show that deletion of the *cle-1* NC1 domain results in cell migration and axon guidance defects. These defects can be rescued by ectopic expression of the NC1 domain, which is shown to trimerize in vitro but not by the monomeric ES domain. Ectopic ES expression dominantly inhibits cell motility, phenocopying the NC1 domain deletion and suggesting that ES inhibits NC1 activity. Similar results for vertebrate type XVIII collagen are reported by Kuo et al. (2001, this issue), and, together, these data suggest that monomeric ES can inhibit the promigratory activities of trimeric NC1.

Materials and Methods

Culture Techniques

C. elegans culture and manipulation were performed using standard methods (Brenner, 1974). All strains were maintained at 20°C. The following strains were used: wild-type N2 var. Bristol, MT2180 *nDf23/unc-13(e1091) lin-11(n566),* and DP19 *unc-119(ed3)*. The following integrated green fluorescent protein (GFP) neural marker strains were used: a pan neuronal marker (*evIs111* [F25B3.3::GFP]), a DA/DB motor neuron marker (*evIs82* [*unc-129*::GFP]), and a mechanosensory neuron marker (*muIs32* [*mec-7*::GFP]).

cle-1 Structure and Expression Constructs

The *cle-1* gene structure was determined by analysis of cDNAs generated by the genome project and sequencing of reverse transcription (RT)–PCR products generated from total *C. elegans* RNA. The *cle-1* isoforms were first reported as three genes (C36B1.2, C36B1.1, and F39H11.4, in 5′ to 3′ order) available from GenBank/EMBL/DDBJ under accession numbers Z80215 and Z81079. The following cDNAs were examined: cm11a3 (Z14325), cm10e6 (M88890), yk96a11 (D75069, D72240), yk297a9 (C26933, C53322), yk12b4 (D27520), and yk238e4 (C61305, C52129). Sequence analysis shows that yk238e4 is a full-length *cle-1B* cDNA and that cm11a3 is a full-length *cle-1C* cDNA containing an SL1 splice leader. All nucleotide numbering is based on cosmid F39H11 sequences annotated with *cle-1* information (AF164959).

The pBA52 (*cle-1A::*GFP) transcriptional reporter was generated by inserting the SalI–BamHI (3703–8654) fragment from cosmid F39H11 into pJJ471. The pJJ471 vector contains the polylinker and synthetic transmembrane domain of pPD34.110 (Fire et al., 1990), followed by GFP from pPD95.75 and an *unc*-54 3′ end cassette. pBA36 (*cle-1B::*GFP) contains a PCR-generated fragment (10996–11969) inserted into the MscI site of pPD116.16. pBA35 (*cle-1C::*GFP) was made by fusing an Nsi1 fragment (17696–20385) to PstI-digested pPD114.35. Descriptions of pPD plasmids are available at www.ciwemb.edu/pages/firelab.html.

For ectopic expression of CLE-1 domains, full-length *cle-1C* cDNA was generated by PCR from cm11a3 using primers SL1 (GGTTTAATTACCCAAGTTTGAG) and cle-1FullR1 (TGGAGCTGACTCATTTTTTGAAGTCGGATG). The product was subcloned into MscI–NheI-digested pPD114.108 (*mec-7::*GFP*::let-838 3′UTR*), replacing the GFP coding sequence. The resulting plasmid was digested with EcoRV and SmaI and religated to make pBA43 (*mec-7*::CelNC1), or digested with Acc65I, blunted by Klenow treatment, and religated to make pBA46 (*mec-7*::CelES). To make *mec-7*::CelAD, pBA43 was digested with BglII and NheI and ligated to the BamHI–XbaI GFP coding fragment from pPD114.35. All clones were sequenced to confirm that they had the expected structure.

Transgenic strains were generated as previously described (Mello et al., 1991). The *cle-1* promoter::GFP expression plasmids (50 μg/ml) were coinjected with the pDP number MM016B [*unc-119*+] plasmid at 100 μg/ml into *unc-119(ed3)* animals. Ectopic expression plasmids at 25 μg/ml were coinjected with pPD114.108 (*mec-7::*GFP) at 25 μg/ml and *tph-1::* GFP at 100 μg/ml (Sze et al., 2000) into N2 wild-type animals. Transformants were identified by GFP expression using a Leica MZ3 fluorescent dissecting microscope. Expression of ectopic NC1 or ES domains was checked by RT-PCR of RNA from transgenic animals using the SL1 and F1NestTGA primers (TCATTTTTTGAAGTCGGATGTG). Only lines showing products of the expected size, 1,340 and 815 nt, respectively, for ectopic CelNC1 and CelES transcripts were analyzed. Transgenic arrays were passed into the *cg120* background by mating to *cg120* males.

Deletion Mutagenesis

Deletion mutagenesis was performed as described (Barstead, 1999) using UV/TMP as a mutagen. Primers used to identify *cg120* were MUTF1 (AACAACAAGCTGCGACAACTCC; 21948–21969), MUTR1 (TCCGGCTACTATCCACAACGAC; 25867–25888), NESTF1 (TGCCCCACCTTCCAATCAATG; 21979–21999), and NESTR1 (CCTCAAATGGGACAACAGCAACC; 25620–25641). The *cg120* deletion was shown to remove nucleotides 22756–24758 by sequencing of PCR fragments derived with primers flanking the deletion. The original mutant strain was out-crossed to wild type 10 times before further analysis.

RNA Interference (RNAi) of cle-1

Double-stranded RNA (dsRNA) was prepared as described (Fire et al., 1998) using the complete yk96a11 cDNA as a template. The resulting dsRNA includes sequences extending from nucleotides 21405–25636 on the genomic sequence. dsRNA was injected at 1 mg/ml into the *evIs82* or the *cle-1(cg120) evIs82* strains. Similar results were obtained using dsRNA at 4 mg/ml.

Microscopy

Microscopy of living animals was performed by mounting on a 2% agarose pad in a small drop of M9 containing 10 μg/ml tetramisole as an anesthetic. Immunohistochemistry of mixed staged cultures (Bettinger et al., 1996) and embryos (Graham et al., 1997) was performed as described. Fluorescent and Nomarski images were obtained using a ZEISS Axoiophot microscope equipped with a Photometrics Sensys charge-coupled device camera. Images were serially deconvolved using MicroTome™ software (VayTek).

Anti–CLE-1 Antibody Production

Primers CE-3 (5′-ATAAGCTTATGGAGCAGCTGCTGATCCAGT-3′) and CE-4 (5′-ATGGTACCTGATGATGGTGTTAGTATGGAA-3′) were used to generate a 469-bp RT-PCR fragment that was cloned into

Published March 19, 2001

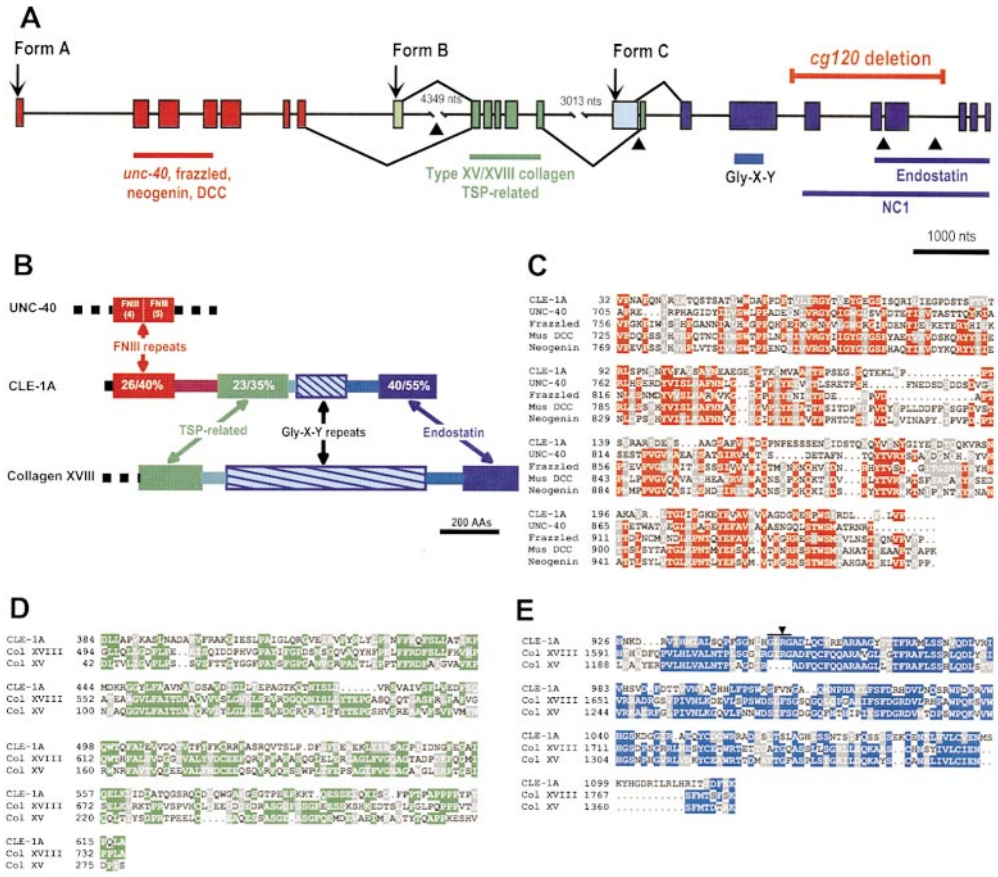

Figure 1. cle-1 Gene and protein structures. (A) Genomic structure of *cle-1* (sequence data available from GenBank/EMBL/DDBJ under accession number AF164959). Exons are indicated as boxes; introns, as lines. Form A–specific exons are red, exons common to forms A and B are dark green, and exons common to all forms are dark blue. The predicted translation start site of each isoform is indicated by an arrow. Splicing patterns for inclusion of the form B– or C–specific first exons (light green or light blue, respectively) are indicated above the intron/exon structure, and splicing patterns for the longer forms, lacking these exons, are below. The four introns that are conserved in *cle-1* and mammalian type XVIII and XV collagens are marked with arrowheads. Extents of CLE-1 protein domains are indicated below the structure, and extents of the *cg120* deletion are indicated above. (B) CLE-1A domain structure and relatedness to mouse type XVIII collagen and *C. elegans* UNC-40. Homologous domains are indicated with the same colors. Percentages of amino acid sequence identity and similarity are indicated in the relevant CLE-1A domains (identity/similarity). The regions connecting the thrombospondin (TSP)-related and ES domains to the Gly-X-Y repeats are 34% similar between CLE-1 and type XVIII collagen. (C) Alignment of CLE-1A fibronectin type III (FNIII) repeats with *C. elegans* UNC-40 (AAB17088), *Drosophila* Frazzled (AAC47314.1), mouse DCC (P70211), and mouse neogenin (CAA70727.1). (D) Alignment of CLE-1A TSP-related motifs with mouse collagen types XVIII (AAC52903) and XV (AAC53387). (E) Alignment of the CLE-1A COOH-terminal domain with mouse ES (Col XVIII) and restin (Col XV). The four amino acid loop containing Arg158 (arrowhead) is present in CLE-1 and type XVIII collagen but not type XV collagen.

KpnI–HindIII-digested vector pQE-41 (QIAGEN), which adds an NH_2-terminal His tag to amino acids 287–439 (CLE-1C). The resulting clone, cecolPQE-41, was transformed into *Escherichia coli* strain M15, and protein expression was performed according to manufacturer's instructions (QIAGEN). Purified fusion protein was used to immunize rabbits. The resulting antisera were affinity purified on columns carrying the purified fusion protein.

Recombinant cle-1 Proteins

CLE-1 NC1 domain sequences were amplified by PCR from cDNA yk234e8 using NC1-5′ (GATCGGCCCAGCCGGCCCATCATCACCATCACCATGACGATGACGATAAGGGAACTGCAGTAAATGTTCATGCAACCACGGTG) and NC1-3′ (GATCGGATCCTTACTTTTTTGAAGTCGGATGTGATTCGATGCAAGC). The CLE-1 ES domain was similarly amplified using ES-5′ (GATCGGCCCAGCCGGCCCATCATCACCATCACCATGACGATGACGATAAGGTTCATAATAAAGATCGAGTTATTCATATGATTGC) and the NC1-3′ primer. The amplified sequences append NH_2-terminal 6xHis tag and enterokinase cleavage sites to the NC1 or ES domains. PCR products were ligated into SfiI–BamHI-digested pSecTag2A (Invitrogen) as an in-frame fusion with the Ig κ secretion signal and the resultant plasmids transfected by calcium phosphate into 293T cells. Conditioned media from transfected 293T cells were purified over Ni–agarose (QIAGEN) and dialyzed overnight into PBS. Purified CLE-1 NC1 and CLE-1 ES proteins were cross-linked with ethylene glycol bis-succinic acid (EGS) and analyzed by SDS-PAGE, followed by Western blotting using anti–CLE-1 antisera.

Results

cle-1 Encodes the C. elegans Type XV/XVIII Collagen Gene

The *cle-1* gene (collagen with ES domain) is the only homologue of vertebrate type XV/XVIII collagens in the *C. elegans* genome. *cle-1* is a complex gene using three promoters and alternative splicing to generate at least three mRNAs designated *cle-1A-C* (Fig. 1). Each CLE-1 isoform has a unique first exon beginning with a predicted signal peptide. All isoforms share the collagenous Gly-X-Y repeat domain and COOH-terminal domain with 55% similarity to mouse ES (Fig. 1, B and E). The CLE-1A and -B forms add a region with 35% similarity to vertebrate type XV/XVIII collagens that is related to the NH_2-terminal thrombospondin domain also found in collagens IX, XVI, and XIX (Fig. 1, B and D). The CLE-1A–specific NH_2-terminal domain contains two fibronectin type III (FNIII) repeats with 40% similarity to the fourth and fifth repeats in the UNC-40/DCC family of netrin receptors (Fig. 1, B and C).

4 introns are located in identical positions in *cle-1* and the mammalian type XVIII and XV collagen genes, indicating that these genes are true homologues. At the amino acid se-

Published March 19, 2001

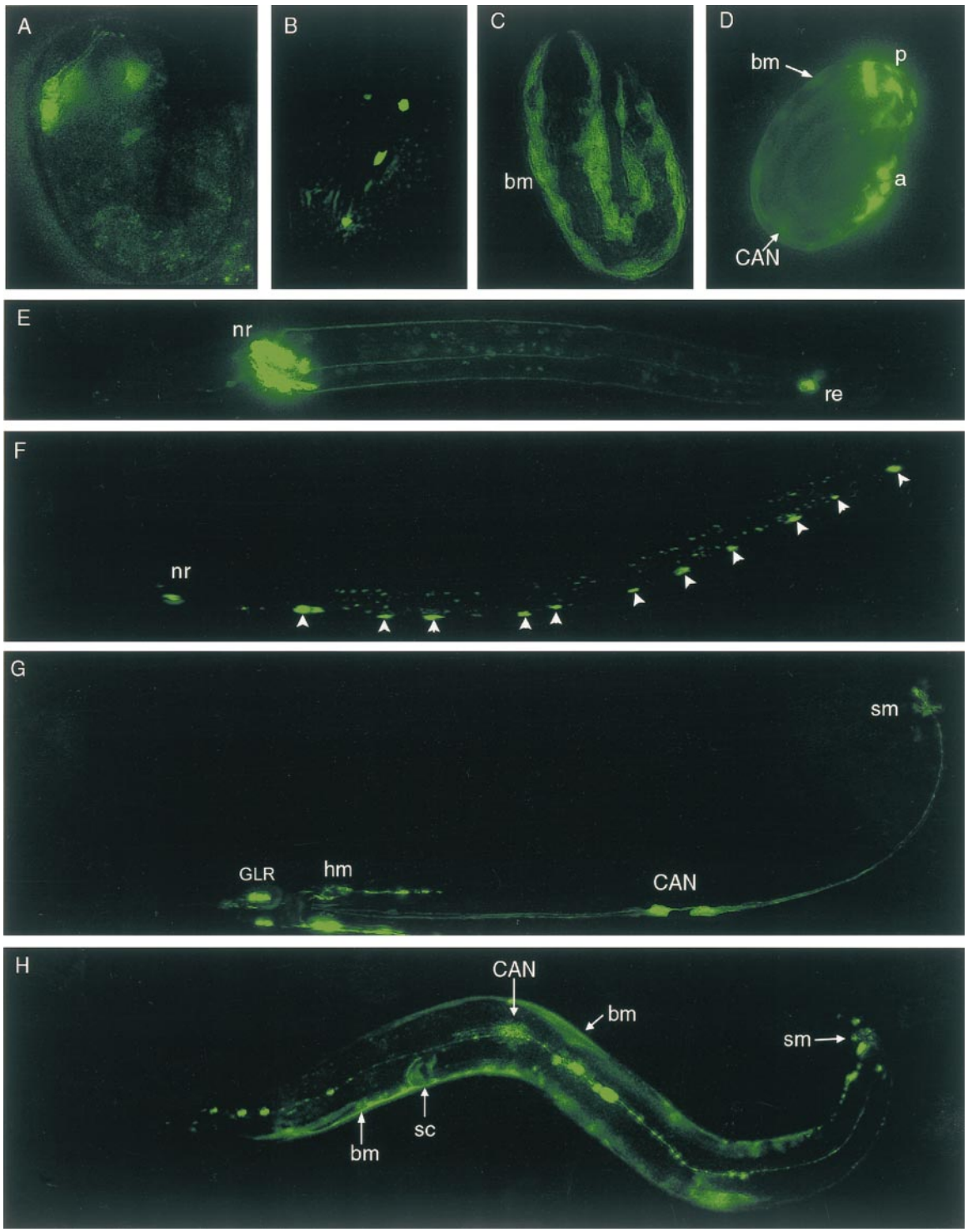

Figure 2. Expression patterns of *cle-1*::GFP transcriptional reporters. Isoform-specific GFP transcriptional reporters show the expression patterns of *cle-1A* (A and E), *cle-1B* (B and F), and *cle-1C* (C, D, G, and H). In A–D, anterior is up and dorsal is to the left; in E–H, anterior is to the left, and dorsal is up. (A) *cle-1A* expression in the cephalic neurons of a 1.75-fold stage embryo. Expression is also seen in S-type interneurons at later stages. (B) *cle-1B* expression in a threefold embryo is seen in DD ventral motorneurons (four are visible and two are out of the plane of focus). This GFP fusion localizes to the nucleus, making axon visualization difficult. (C) *cle-1C* expression in the body wall muscles (bm) of a twofold embryo. Pharyngeal expression is not seen in this focal plane. (D) In a threefold embryo, *cle-1C* expression in body wall muscles is weaker, but strong expression is seen in pharyngeal cells (p), accessory muscles, some unidentified cells near the anus (a), and the canal-associated neurons (CAN). (E) In an L2 larva, *cle-1A* expression is strong in the nerve ring (nr) and rectal epithelial cells (re). GFP is weakly detected in axons of the S-type interneurons that run sublaterally. (F) *cle-1B* expression in dorsal motorneuron cell bodies (arrowheads) located along the ventral nerve cord of an L2 larva. Faint GFP activity can be detected in commissural axons of most animals. (G) *cle-1C* expression in an L2 larva is limited to a subset of glial-like GLR cells, the head mesodermal cell (hm), the canal-associated neurons, and weakly in the anal sphincter muscle (sm). (H) *cle-1C* expression in adult body wall muscles (bm), accessory muscles (sm), canal associated neurons (CAN), and gonadal sheath cells (sc).

Published March 19, 2001

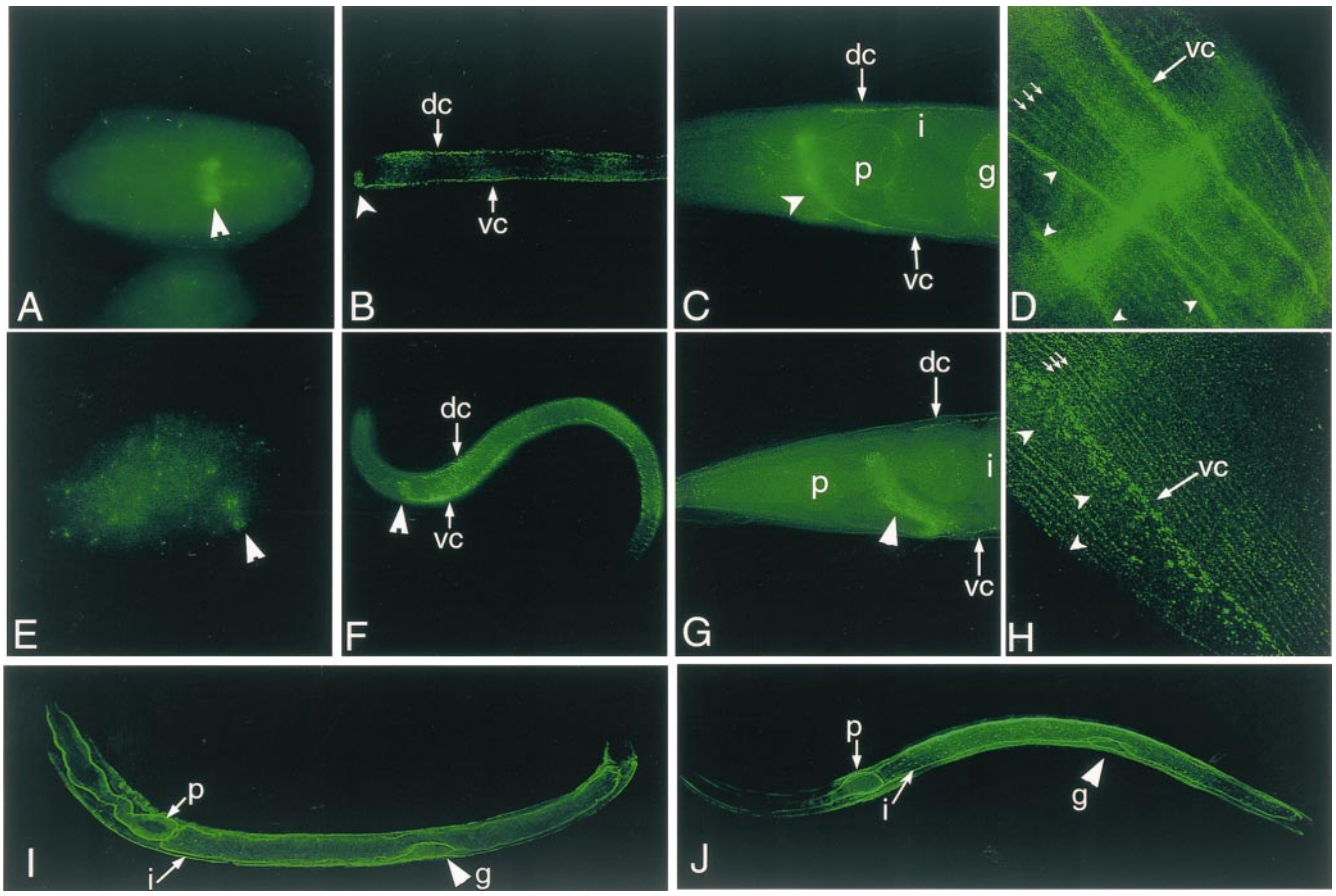

Figure 3. Localization of CLE-1 and type IV collagen in wild-type and *cg120* animals. Immunofluorescent localization of CLE-1 (A–H) and type IV collagen (I and J) are shown in wild-type (A–D and I) and *cg120* (E–H and J) animals. In all panels, anterior is left, and dorsal is up. (A) A fourfold embryo shows strong CLE-1 staining associated with the nerve ring (arrowhead). (B) In larval animals, CLE-1 accumulates on the nerve ring (arrowhead) and the dorsal (dc) and ventral (vc) nerve cords. (C) In adults, staining for CLE-1 is strong on the nerve ring and nerve cords (dc and vc) and is weakly detected on the surfaces of the pharynx (p), intestine (i), and gonad (g). (D) Under body wall muscle of an adult, CLE-1 accumulates strongly at the junctions between muscle cells (arrowheads) and along muscle-dense body lines (small arrows) but is not coincident with the dense bodies. Staining on the ventral nerve cord is distinctly punctate. (E) Weak CLE-1 accumulation on the nerve ring of a *cg120* embryo. (F) CLE-1 localization to the nerve ring (arrowhead) and dorsal (dc) and ventral (vc) nerve cords of a *cg120* larva. (G) Accumulation on nerve ring (arrowhead), nerve cords (dc and vc), pharynx (p), and intestine (i) of a *cg120* adult. (H) Under the body wall muscle of a *cg120* adult, CLE-1 accumulates along dense body lines (small arrows) and along the ventral nerve cord (vc) as in wild type. However, there is no accumulation at the junctions between muscle cells (arrowheads), and the pattern on the nerve cord is more diffuse. (I and J) Wild-type and *cg120* L1 larvae show type IV collagen localization in the basement membranes of the pharynx (p), intestine (i), and gonad primordium (g).

quence level, CLE-1 is equally similar to types XV and XVIII collagen. However, both *cle-1* and vertebrate type XVIII collagen are expressed as three isoforms (Muragaki et al., 1995; Rehn and Pihlajaniemi, 1995), whereas type XV has no identified isoforms. Also, both the CLE-1 and vertebrate type XVIII collagen ES domains have a four–amino acid loop (Fig. 1 E) that is not present in type XV (Sasaki et al., 2000). This loop contains Arg158 and has been shown to contribute strongly to the heparin binding property of ES (Sasaki et al., 1998). Based on these comparisons, we conclude that CLE-1 is most similar to type XVIII collagen. The most notable difference is that the type XVIII collagen NH_2-terminal domain contains a region related to the Wingless receptor *frizzled*, whereas the equivalent CLE-1 domain is related to the netrin receptor *unc-40* (Chan et al., 1996).

cle-1 Isoforms Are Differentially Expressed

cle-1 expression was analyzed in transgenic animals carrying GFP transcriptional reporters driven by sequences upstream of the unique first exon of each isoform. *cle-1A*::GFP expression was first detected in comma stage (~390 min) embryos in cephalic neurons (Fig. 2 A). Expression in interneurons and rectal epithelial cells is seen by the twofold stage, ~60 min later, and continues through larval and adult stages (Fig. 2 E). *cle-1B*::GFP expression was first observed at the threefold stage (~520 min) of embryogenesis in four neurons of the lateral ganglia and in the DD dorsal motorneurons (Fig. 2 B). The postembryonic VD dorsal motorneurons also express *cle-1B*::GFP starting in the second larval stage, and this pattern persists through larval and adult stages (Fig. 2 F).

cle-1C::GFP expression is first seen in comma stage embryos in pharynx and body wall muscles (Fig. 2 C) and later appears in the canal-associated neurons (CAN), head mesodermal cell, accessory muscles, and intestine (Fig. 2 D). During larval development, expression is restricted to the ventral GLR glia–like cells, the canal-associated neurons, and the head mesodermal cell (Fig. 2 G). Beginning in the

Published March 19, 2001

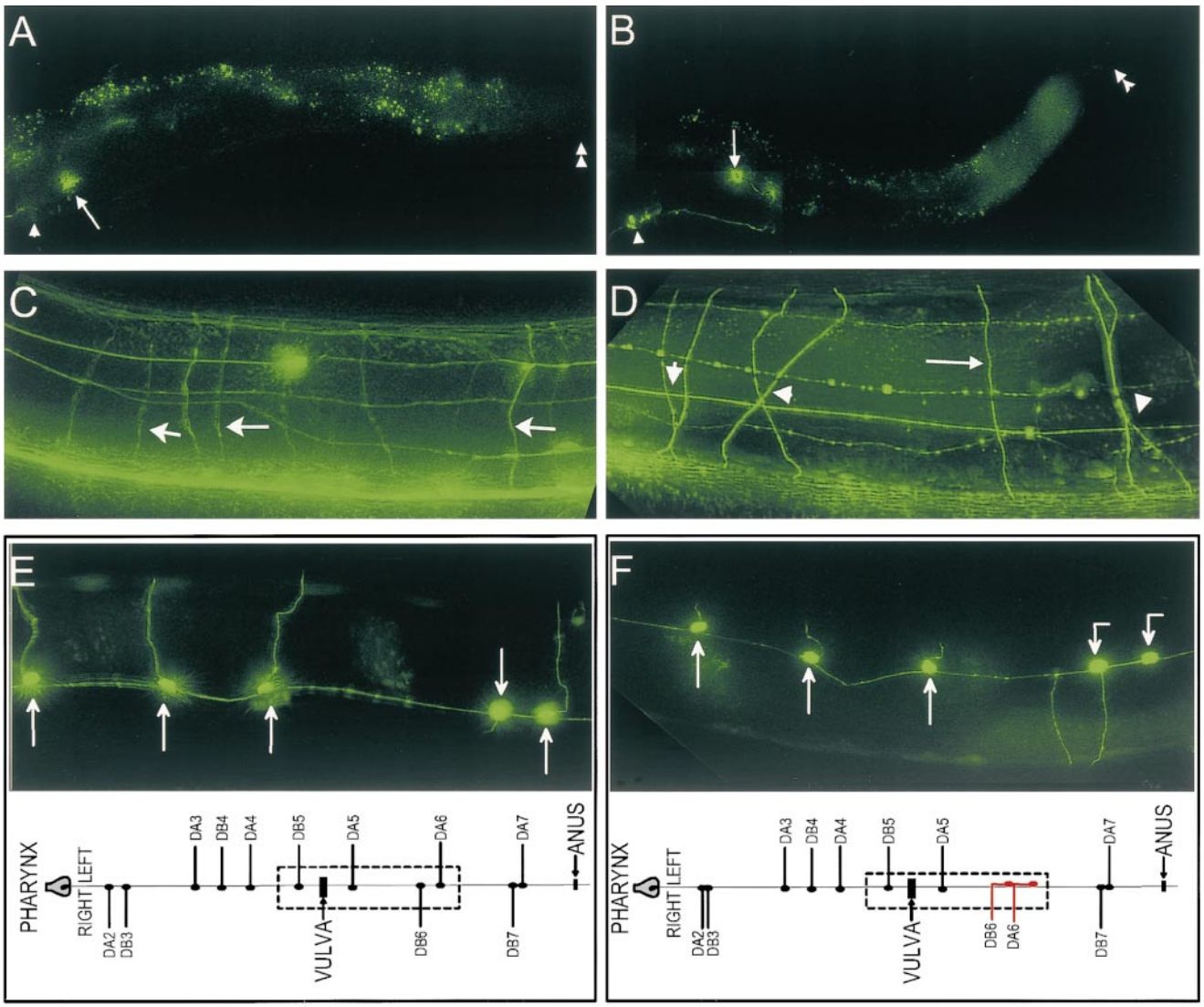

Figure 4. Cell and axon migration defects in *cle-1(cg120)* animals. Cell and axon positions were analyzed in wild-type (A, C, and E) and *cg120* mutant (B, D, and F) animals. Anterior is left, and dorsal is up in all panels. (A and B) HSNs visualized using the *tph-1*::GFP marker (Sze et al., 2000) are indicated with an arrow. The positions of the vulva (arrowhead) and anus (double arrowhead) are marked to visualize the relative position of the HSN. (A) In wild-type animals, the left HSN is positioned immediately posterior of the vulva. (B) In this *cg120* animal, the HSN is displaced posteriorly and dorsally. The HSN axon abnormally projects posteriorly and then ventrally to the ventral cord. (C and D) A panneuronal marker (F25B3.3::GFP) was used to visualize the general organization of the nervous system. (C) In wild-type animals, dorsoventral axon migrations (arrows) follow a trajectory that is orthogonal to the anterior–posterior axis. (D) Axons in *cg120* mutants frequently follow nonorthogonal trajectories and defasciculate from one another (arrowheads), but some axon trajectories are normal (arrow). (E and F) Visualization of DA and DB motorneurons using the *unc129*::GFP reporter. Schematics of the complete DA and DB cell body and axon patterns are shown below, and the area shown in the micrographs is boxed with a dashed line. (E) In wild-type animals, the DA and DB motorneurons extend commissural axons directly from their cell bodies. (F) In this *cg120* animal, the DA6 and DB6 axons abnormally migrate anteriorly along the ventral cord, and then both exit on the right side. The DA6 axon should exit on the left side of the ventral cord.

late fourth larval stage and continuing through adult, *cle-1C*::GFP expression appears in somatic sheath cells of the gonad and reappears in body wall muscles (Fig. 2 H).

CLE-1 Protein Accumulates Strongly on the Nervous System

Anti–CLE-1 antiserum was raised against a region common to all isoforms and used to localize the protein in whole animals. CLE-1 strongly accumulates in a punctate pattern associated with the nerve ring and the dorsal and ventral nerve cords. This pattern is first visible at the two-fold stage of embryogenesis (~460 min) and persists in all subsequent stages (Fig. 3). Beginning in the L4 larval stage, CLE-1 is also observed in basement membranes surrounding the gonad, pharynx, and intestine (Fig. 3 C), and under body wall muscles where it preferentially accumulates at junctions between muscle cells and along dense body lines (Fig. 3 D). The apparently more limited distribution of CLE-1 in early development may result from low sensitivity of detection with the antibody.

Published March 19, 2001

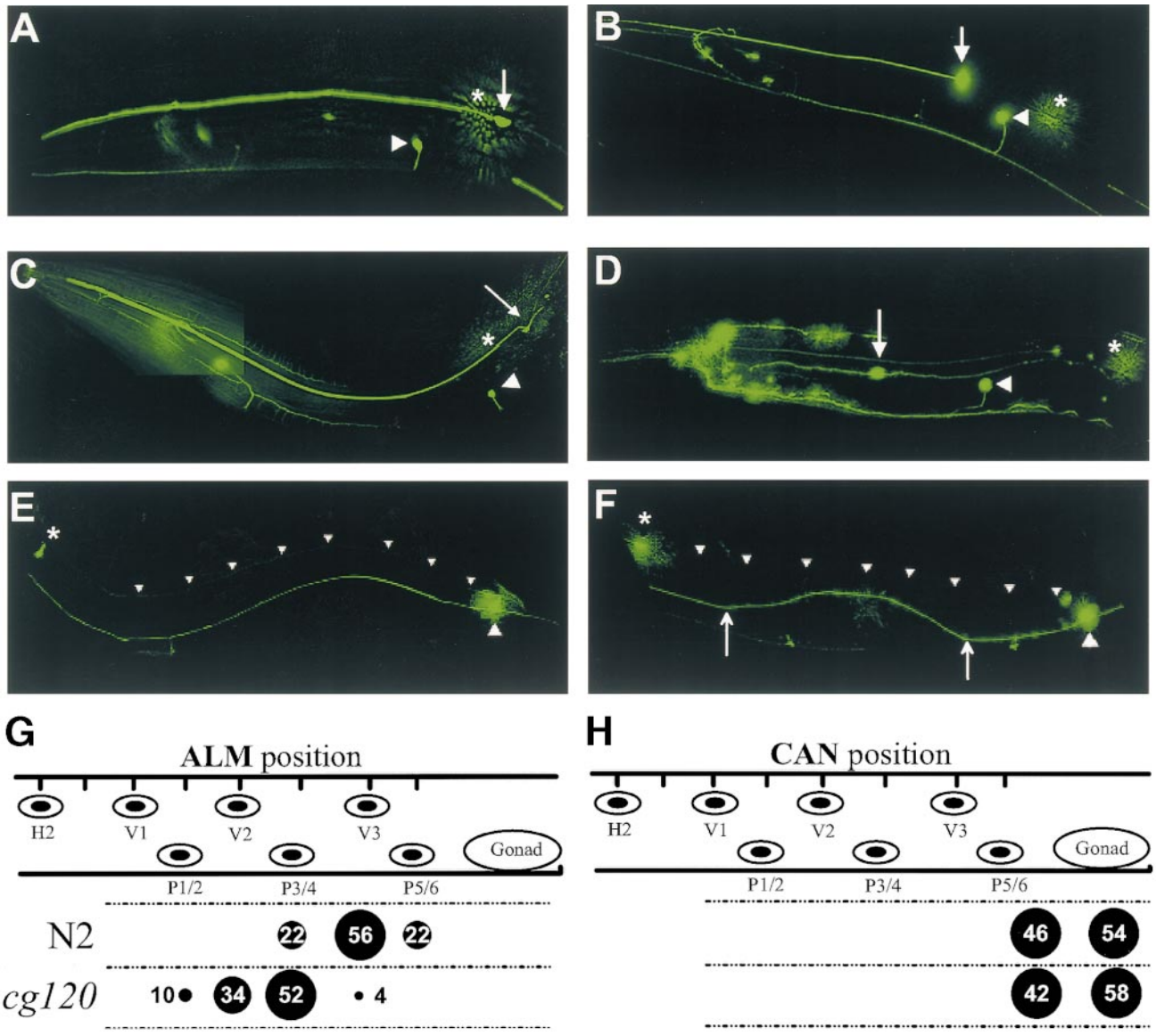

Figure 5. Cell positioning and axon guidance of mechanosensory neurons. The *mec-7*::GFP marker was used to visualize the anterior (A–D) or posterior (E–F) mechanosensory neuron cell bodies and axons. Anterior is left, and dorsal is up in all panels. (A) In wild-type animals, ALMR (arrow) is located posterior and dorsal of AVM (arrowhead). ALML (*) is out of the plane of focus. (B) In a *cg120* mutant, ALMR (arrow) is located anterior of AVM (arrowhead), whereas ALML (*) is normally positioned. (C) In a *cg120* animal expressing *mec-7*::CelNC1, the anterior mechanosensory neurons are normally positioned. (D) In a wild-type animal expressing *mec-7*::CelES, ALMR (arrow) is located both anterior and ventral of its normal position, whereas ALML is normally positioned. (E and F) PLM cell bodies are not mispositioned in *cg120*, so their axons were analyzed for guidance defects. (E) In wild-type animals, the PLMR axon (large arrowhead) extends anteriorly along the sublateral tract and terminates just posterior of the ALMR cell body (*). The dorsal edge of the animal is indicated (small arrowheads). (F) In a *cg120* animal, the PLMR axon deviates dorsally from the normal ventral sublateral position over a segment of its path (arrows). (G and H) The positions of ALM mechanosensory neurons (G) and canal-associated neurons (CAN; H) were scored in first larval stage animals immediately after hatching using differential interference contrast optics. Cell positions were scored relative to the hypodermal nuclei, which are represented by ovals in the upper part of the drawing. These nuclei are in fixed positions and are used as static markers to score cell positions. Numbers and circles in the lower part of the drawing indicate the percent of animals ($n = 50$) with cells in the indicated positions.

The cle-1(cg120) Allele Deletes the NC1 Domain

We isolated a deletion of *cle-1*, *cg120*, which removes exons 18–20 and places the final three exons out of frame (Fig. 1 A). This deletion results in CLE-1 proteins lacking the COOH-terminal 231 amino acids, which includes nearly the entire COOH noncollagenous NC1 domain. CLE-1 protein is detectable in *cg120* animals by immunofluorescence (Fig. 3, E–H), demonstrating that stable truncated protein is produced.

CLE-1 localizes to the nerve cords, nerve ring, pharynx, intestine, and gonad of *cg120* animals in a pattern similar to wild type (Fig. 3, E–H). However, the intensity of CLE-1 staining is reduced in *cg120*, presumably because 45% of the region used as immunogen is removed by the deletion,

Published March 19, 2001

Table I. Cell Position Defects of cle-1 Mutant- and Ectopic-expressing Strains

Background	N	Transgene	ALML*	ALMR	AVM	HSN§
N2	162	—	7.7‡	1.4	1.1	2.0
N2	200	*mec-7::CelNC1*	3.0	1.8	1.3	ND
N2	108	*mec-7::CelES*	20.0	23.0	2.0	ND
N2	50	*mec-7::CelAD*	8.0	6.0	2.0	ND
cg120	220	—	31.5	20.0	25.0	27.0
cg120	128	*mec-7::CelNC1*	6.6	3.0	2.2	ND
cg120	50	*mec-7::CelES*	32.0	18.0	14.0	ND
cg120	50	*mec-7::CelAD*	34.0	26.0	12.0	ND

*ALML, ALMR, and AVM positions were scored using the *mce-7::GFP* reporter.
‡Numbers indicate percentage of animals displaying mispositioned cells.
§HSN positions were scored using the *tph-1::GFP* reporter. 250 HSNs were scored for both N2 and *cg120*.

Table II. Axon Guidance Defects of cle-1 Mutant- and Ectopic-expressing Strains

Background	N	PLM*	DA/DB‡	DA/DB§
N2	100	2.0	4.0	2.0
cg120	100	12.0	35.0	15.0
cle-1 RNAi	100	ND	16.0	7.0

*Percentage of animals having mispositioned PLM axons.
‡Percentage of animals displaying abnormal anterior/posterior migrations of DA/DB axons.
§Percentage of animals that show one or more DA/DB axons exiting from the wrong side of the ventral nerve cord.

and/or the truncated protein is less stable. Also, the accumulation of CLE-1 at the junctions between body wall muscle cells is absent from *cg120* animals (Fig. 3 H), suggesting that the NC1 domain is necessary for this localization.

Type IV Collagen Distribution Is Normal in cg120 Mutants

To determine whether there is general disruption of basement membranes in *cg120* animals, we examined the distribution of type IV collagen, a major basement membrane component. The collagen IV distribution in *cg120* mutants was indistinguishable from wild type (Fig. 3, I and J), and, when normalized to myosin staining, collagen IV levels in the mutants were equivalent to wild type. Type IV collagen assembly appears unaffected by the *cg120* deletion, suggesting that general basement membrane structure is not disrupted.

Deletion of the cle-1 NC1 Domain Causes Multiple Defects

30% of *cg120* deletion homozygotes are egg-laying defective (Egl), 30% display distal tip cell migration defects resulting in mispositioned gonad arms, 10% have male tail defects, and they generally display slightly incoordinated movement (Unc). In addition, 1–5% arrest as late embryos or first stage larvae (L1). These phenotypes can be found in various combinations in single animals. The frequency of embryonic or larval arrest increases to ~35% in animals with *cg120* in trans to a deficiency of the region, *cg120/nDf23*, consistent with the antibody staining results in demonstrating that *cg120* is not a null allele.

Neural Migration and Axon Guidance Defects in cg120 Mutants

The Egl phenotype can arise from defects in migration or function of either the hermaphrodite-specific neurons (HSNs) that control egg laying or the sex myoblasts that generate the egg laying musculature. These cells normally migrate from the tail to the midbody region, near the presumptive vulva (Garriga et al., 1993; Burdine et al., 1997). Egl defects can be classified as neuronal or muscular by examining egg laying in response to serotonin or imipramine treatment (Desai and Horvitz, 1989). Egg laying by *cg120* animals was strongly stimulated by serotonin treatment but only variably stimulated by imipramine, consistent with impaired HSN neural function (data not shown).

HSN positions were visualized in adults using a tryptophan hydroxylase GFP marker that is expressed in these cells (Sze et al., 2000). In 27% (n = 250) of *cg120* animals one or both HSNs were located significantly posterior and/or dorsal of their normal position, suggesting that they failed to complete migration from the tail (Fig. 4 B). HSN axon guidance defects were also observed in *cg120* animals but may be secondary effects of cell mispositioning (Baum and Garriga, 1997). Animals displaying the Egl phenotype generally had mispositioned HSNs, suggesting that the Egl phenotype results from the HSN migration defect.

In addition to HSNs, other cells that undergo long range migrations during *C. elegans* development include the anterior mechanosensory neurons (ALML/R and AVM) and the canal-associated neurons. We analyzed these cells for migration defects in *cg120* mutants (Fig. 5; Tables I and II). Interestingly, although the canal-associated neuron is the only one of these cells that expresses *cle-1*, it did not exhibit any migration defects (Fig. 5 J). In 37% (n = 200) of *cg120* animals one or more of the mechanosensory neurons were mispositioned (Fig. 5 B; Table I). The ALMs are most often displaced anteriorly, whereas the AVM is displaced posteriorly and/or dorsally. In most cases the cells are mispositioned on the anterior–posterior trajectory along which they normally migrate, although occasionally they are also displaced dorsally or ventrally.

Axon guidance defects are also detected in *cg120* animals. In wild-type animals, sensory and motor axons migrate orthogonally to the longitudinal axis to innervate the ventral or dorsal nerve cords (Fig. 4 C). In *cg120* mutants, these migrations are frequently defective (32%; n = 50), with axons migrating at oblique angles, crossing one another, or defasciculating from axon bundles (Figs. 4 D and 5 F). These defects may partially explain the mild uncoordination of *cg120* animals.

Defects in axon guidance for the DA and DB motorneurons were specifically visualized using an *unc-129*::GFP reporter (Colavita et al., 1998). The cell bodies of these motorneurons are located in the ventral cord and extend axons along the body wall to the dorsal cord. In wild type, these axons exit directly from the cell body and do not extend along the ventral cord. In 35% (n = 100) of *cg120* animals, axons abnormally exit the ventral cord at some distance from the cell body (Fig. 4 F; Table II). Particular DA and DB axons exit the ventral nerve cord on the right or left side in a stereotypic pattern. In 15% (n = 100) of *cg120* animals, one or more axons exit the ventral cord on the incorrect side of the animal.

Published March 19, 2001

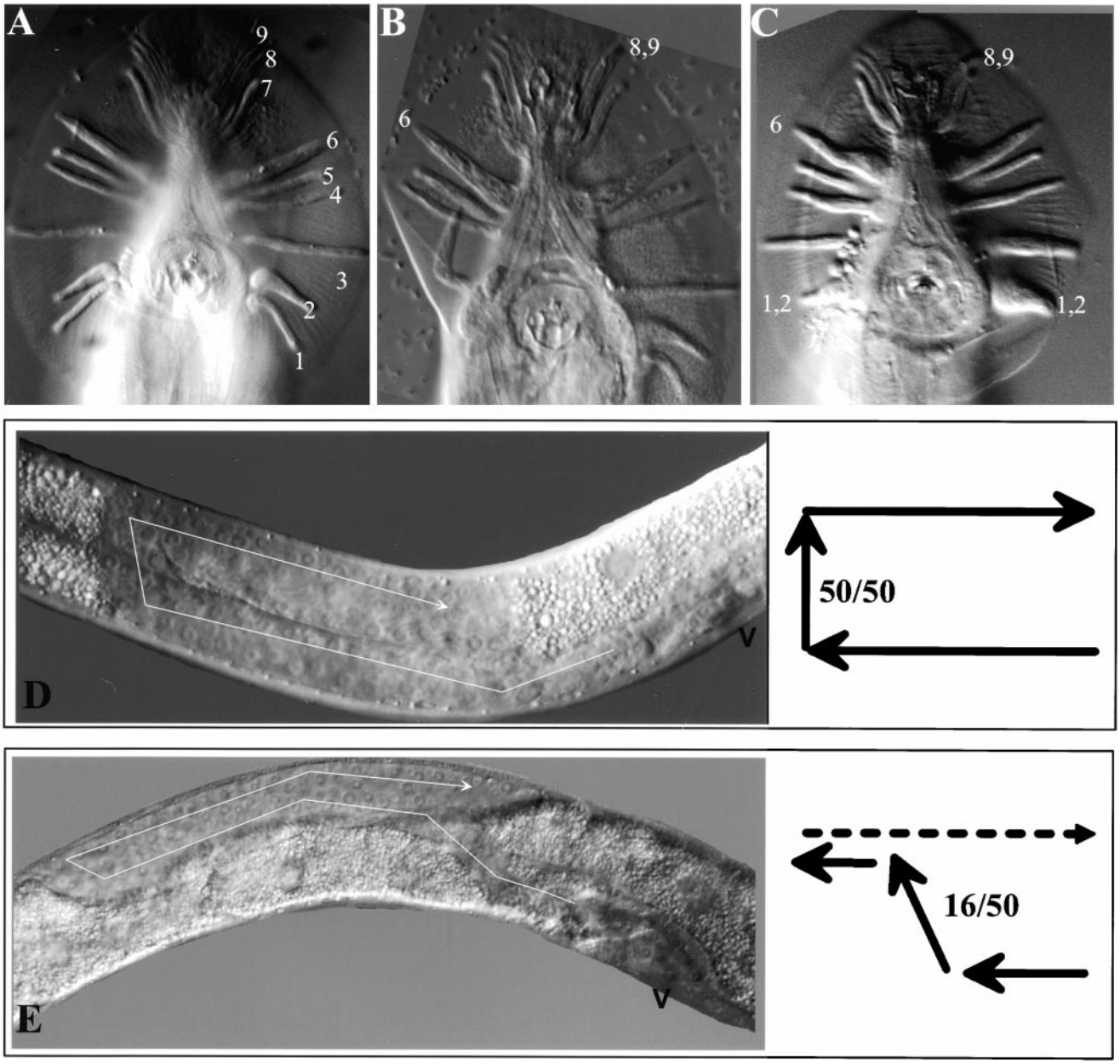

Figure 6. Male tail and gonad migration defects. Defects in morphogenesis of the male tail (A–C) and the hermaphrodite gonad (D and E), visualized with differential interference contrast microscopy. (A) Ventral view of a wild-type male tail showing the nine bilateral pairs of sensory rays, labeled 1–9, on the left side of the animal. (B) A *cg120* male tail shows fusion of rays 8 and 9 (8,9). On the right side, ray 6 is broader than normal, and the cuticle covering it is irregular. (C) The tail of a male ectopically expressing *mec-7*::CelES shows fusion of rays 1 and 2 (1,2) on both sides of the animal. Ray 6 on the right side (6) appears crumpled, and rays 8 and 9 on the left have fused (8,9). The fans and rays of males expressing *mec-7*::CelES are smaller than those of wild type. (D) The anterior arm of a wild-type fourth larval stage hermaphrodite gonad. The distal tip cell (DTC) leads gonad migration anteriorly along the dorsal body wall, turns and migrates to the dorsal side, and then migrates posteriorly. The position of the vulva (V) is indicated. A schematic depiction of the DTC migration path is shown to the right of the micrograph. 100% (50/50) of wild-type animals showed this migration pattern. (E) In this *cg120* animal, the DTC migrated anteriorly, turned dorsal prematurely while continuing to migrate anteriorly, and then reflexed and migrated posteriorly (dashed line) along the dorsal body wall. The final posterior migration is below the plane of focus. 32% (16/50) of *cg120* animals displayed similar migration defects of the anterior gonad. 16% of posterior gonads showed the same defects.

cg120 Animals Exhibit Male Tail and DTC Migration Defects

cg120 animals also display defects in migrations of non-neuronal cells of the male tail and the hermaphrodite gonad. Formation of the male tail involves complex cell migrations and interactions (Sulston et al., 1980; Emmons, 1992). 10% (n = 50) of *cg120* males show fusions of sensory rays 1–2 or 7–8–9, and sensory ray 6 is often short and broad (Fig. 6 B). Despite these defects, most *cg120* homozygous males can mate. In the hermaphrodite gonad, the most common defect (32%) is a premature dorsal turn of the anterior distal tip cell (Fig. 6 E). The posterior gonad shows similar defects with lower frequency (16%).

Published March 19, 2001

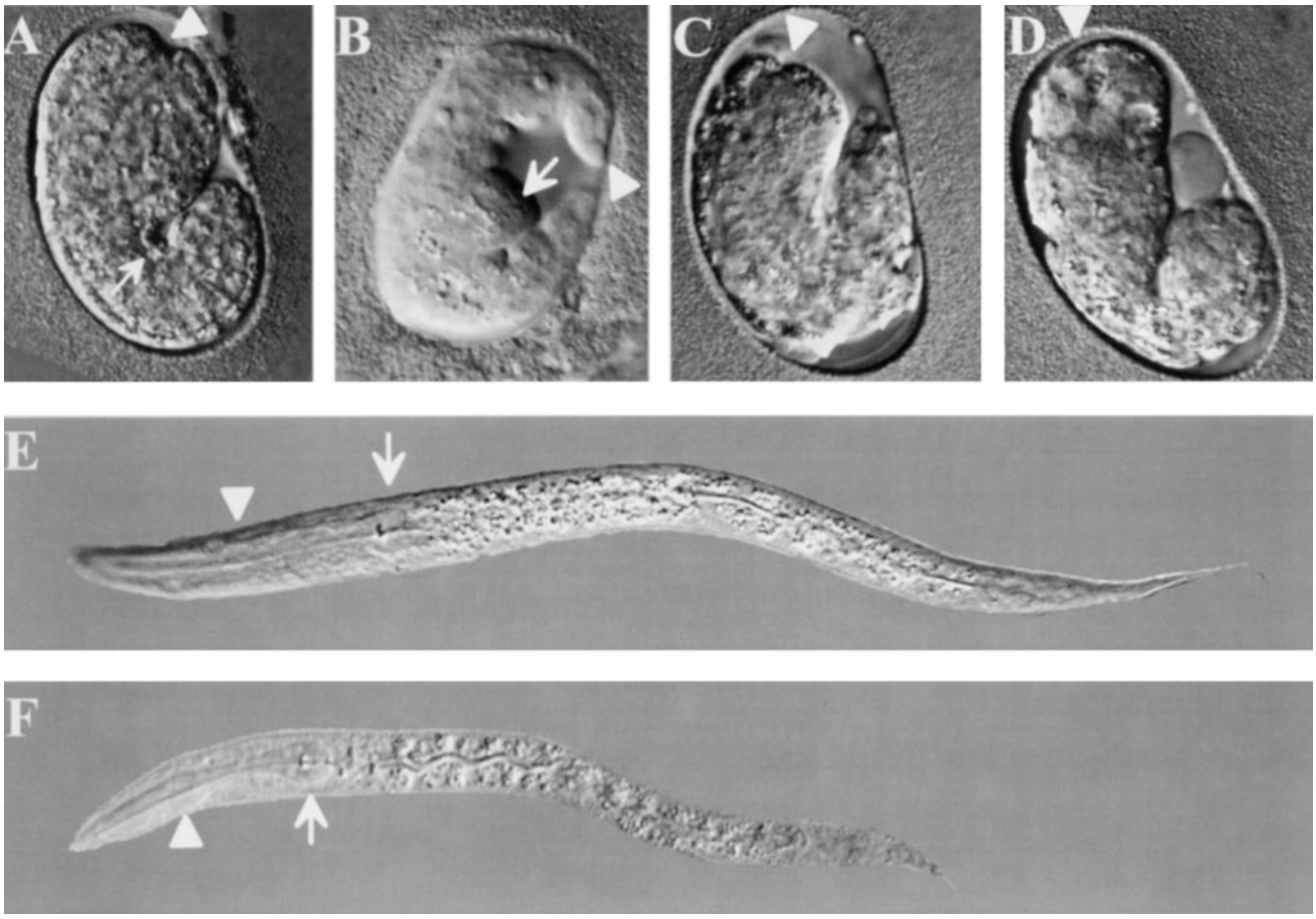

Figure 7. RNAi against *cle-1* results in embryonic and larval lethality. (A–D) Embryonic lethality resulting from RNAi against *cle-1*. Embryos are oriented with anterior up and ventral to the right. The position of the presumptive oral cavity is indicated by an arrowhead. (A) A wild-type embryo at the 1.5-fold stage of embryogenesis. (B) An embryo arrested at the 1.5–2-fold stage of embryogenesis resulting from RNAi into the wild-type background. The embryo has herniated at the ventral pocket (arrow), which forms during enclosure by the hypodermis. (C and D) Embryos arrested at the 1.5-fold stage of embryogenesis resulting from RNAi into the *cg120* background. The embryos are small and misshapen, suggesting defects in hypodermal function. (E and F) Larval lethality resulting from RNAi against *cle-1*. The posterior bulb of the pharynx is indicated by an arrow, and the anterior bulb by an arrowhead. (E) Wild-type first stage larva. The body has a uniform diameter along its length, and the pharynx lies along the central axis of the animal. (F) Arrested first stage larva resulting from RNAi into the wild type background. The animal is smaller than wild type, and the posterior body is shrunken relative to the anterior. The pharynx is mislocalized laterally and does not pump.

Gonads are also often slightly shortened relative to wild type, suggesting that the distal tip cells do not migrate completely along the anterior–posterior axis.

RNAi of cle-1 Results in Pleiotropic Defects

As an independent means of assessing the effects of loss of *cle-1* function, we performed RNA interference (RNAi) against the gene. RNAi has been shown to cause loss-of-function phenotypes for numerous *C. elegans* genes (Fire et al., 1998). We injected dsRNA generated from a region of *cle-1* that is common to all three isoforms and analyzed the resulting phenotypes.

Significant levels of both embryonic and larval lethality were seen in offspring from hermaphrodites injected with *cle-1*-specific dsRNA (Fig. 7; Table III). Embryonic arrest most commonly occurred during early morphogenesis, at approximately the 1.5-fold stage. Larval arrest occurred at the first larval stage, and arrested larvae were small and had misshapen pharynxes that failed to pump. Animals that survived to the adult stage had motorneuron positioning and axon guidance defects (Table II), gonad migration, or male tail defects and were sterile (Table III). These defects are similar to those observed in *cg120* mutants. Injection of dsRNA into *cg120* mutant animals resulted in higher levels of lethality and sterility (Table III). The occurrence of similar phenotypes, but at higher penetrance in RNAi-treated versus *cg120* mutant animals, suggests that RNAi results in greater *cle-1* loss-of-function than the *cg120* deletion.

Ectopic NC1 Domain Expression Rescues Mechanosensory Cell Migration Defects

The *cg120* deletion removes the NC1 domain that consists of three subdomains, an association domain, a hinge region, and the ES domain. To further investigate the functions of these subdomains, we ectopically expressed the full NC1, the association domain, and hinge regions, or the ES domain in wild-type and *cg120* backgrounds. Secreted CLE-1 domains were expressed in mechanosensory neurons using the *mec-7* promoter, which has been previously

Published March 19, 2001

Table III. RNAi of cle-1 in Wild-type and cg120 Backgrounds

	Wild type*		*cle-1 (cg120)*‡	
Defects observed	%	N	%	N
Lethality				
embryonic arrest	18	1,152	25	884
L1 larval arrest	7	1,152	14	884
Sterility§	11	88	20	100
Gonad migration‖	15	88	ND**	ND
Male tail abnormal¶	50	12	ND	ND

Both backgrounds contain *evIs828*; *him-5(e1490)*.
*Totals are from 15 injected hermaphrodites.
‡Totals are from 13 injected hermaphrodites.
§Severe disorganization of the germline, resulting in a lack of viable embryos.
‖Gonad migration defects were similar to those seen in *cg120*.
¶Male tail morphological defects were similar to those seen in *cg120*.
**The penetrance of these defects were not quantified, but were similar to those seen in *cg120*.

used to analyze cell and axon guidance (Hamelin et al., 1993; Colavita and Culotti, 1998). The mechanosensory neuron mispositioning caused by *cg120* was rescued by ectopic NC1 expression, with the frequencies of specific cell position defects reduced 5–10-fold (Table I). In contrast, expression of the ES domain or the association–hinge region did not rescue these migration defects. Other *cg120* phenotypes, such as egg-laying and gonad migration defects, were not rescued by NC1 expression in mechanosensory neurons, possibly due to a limited range of action of the NC1 domain.

Ectopic Endostatin Expression Phenocopies cg120 Migration Defects

Ectopic expression of the ES domain in the wild-type background caused dominant cell position defects, similar to *cg120* mutants (Table II). The mechanosensory neurons were generally mispositioned along their normal trajectories but short of their normal final positions (Fig. 5 D; Table I). Eight independent ectopic ES–expressing transgenic lines showed similar defects with variable penetrance, suggesting that the effect may be dosage sensitive. Ectopic NC1 or association–hinge domain expression in the wild-type background showed no effect on mechanosensory neuron positioning (Table I), indicating that the complete NC1 domain and the ES domain are functionally distinct.

Ectopic ES also affected cells that did not express it. Expression of the ES but not the NC1 domain in mechanosensory neurons resulted in distal tip cell migration defects in 40% of hermaphrodite gonads and tail defects in 30% of males ($n = 50$) (Fig. 6 C). In both cases, the defects are similar to those seen in *cg120* animals, again indicating that NC1 deletion and ectopic ES expression cause similar defects. The distal tip cells and cells of the male tail do not express the ectopic ES, indicating that it acts cell nonautonomously to affect their function.

The C. elegans NC1 Domain Trimerizes In Vitro

A major functional difference between type XVIII collagen NC1 and ES domains is the ability of NC1 to oligomerize (Sasaki et al., 1998; Kuo et al., 2001, this issue). Recombinant CLE-1 NC1 domains expressed in human embryonic kidney 293 cells were found to form trimers (Fig. 8 A), whereas CLE-1 ES domains remained monomeric. Thus, the *C. elegans* domains behave similarly to the mammalian domains in regards to oligomerization, suggesting that the functional differences between ectopically expressed CLE-1 NC1 and ES domains may reflect differences in their ability to oligomerize via the association domain.

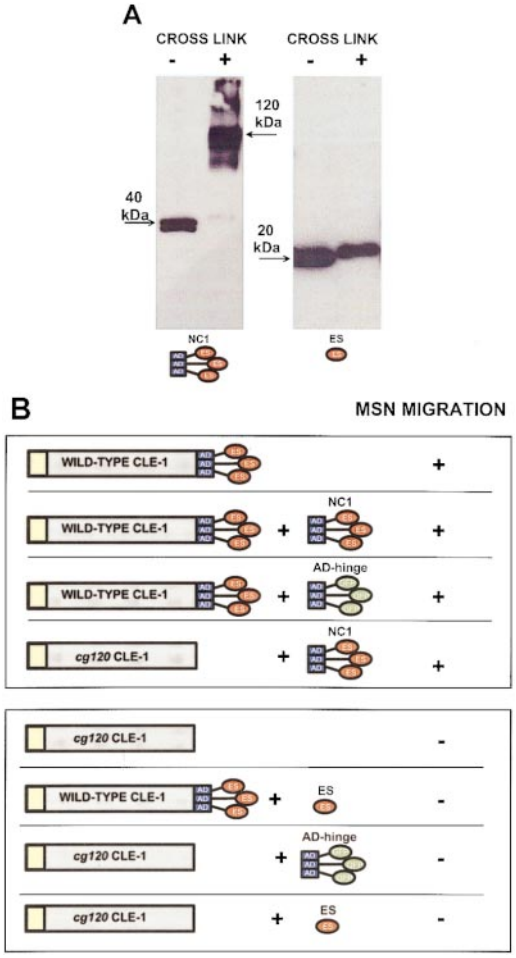

Figure 8. The *C. elegans* NC1 domain trimerizes in vitro. (A) Purified CLE-1 NC1 (left) and ES domains (right) were analyzed by denaturing gel electrophoresis and Western blotting, either before (−) or after (+) cross-linking with EGS. After cross-linking, the 40-kD NC1 monomer migrates at ~120 kD, indicating that it exists as a trimer. The mobility of the ES domain does not shift after EGS treatment, indicating that it exists as a monomer. (B) Summary of mechanosensory neuron migration data. Defective mechanosensory neuron migrations are observed when the NC1 domain is removed by the *cg120* deletion. These defects can be rescued by ectopic NC1 domain expression. In contrast, ectopic ES domain expression causes mechanosensory neuron migration defects in the wild-type background and fails to rescue the NC1 deletion defects. Expression of the association domain and hinge regions fused to GFP, rather than ES, does not rescue *cg120* migration defects and does not cause defects in the wild-type background.

Discussion

We have identified *cle-1* as the homologue of vertebrate type XVIII collagen in the avascular nematode *C. elegans*. Although there are some 150 collagen genes in *C. elegans*

Published March 19, 2001

and more than 20 in vertebrates, only types IV and XVIII are conserved between them (Kramer, 1997; Hutter et al., 2000). We have demonstrated that deletion of the COOH-terminal NC1 domain from the *C. elegans* type XVIII collagen homologue *cle-1* allows for assembly of the truncated protein in basement membranes and does not result in gross disruption of basement membrane structure. Loss of the NC1 domain causes migration defects of multiple cells and axons. Particular migration defects can be rescued by ectopic expression of the complete NC1 domain, but not by its ES subdomain. In fact, ectopic ES expression causes migration defects similar to those resulting from the NC1 domain deletion, suggesting that ES may interfere with NC1 domain function. Similar antagonistic roles of type XVIII collagen NC1 and ES domains on cell migration have been described for vertebrate cells in culture (Kuo et al., 2001, this issue). Conservation of type XVIII collagen across these distant phyla indicates that, like type IV collagen, it is a fundamental matrix component that has conserved functions.

The three isoforms of CLE-1 differ in their domain compositions and their temporal and spatial expression patterns. Notably, the CLE-1A and B isoforms are expressed only in neurons. CLE-1 is broadly distributed in *C. elegans* basement membranes but accumulates to highest levels in association with the nervous system. The elements of the *C. elegans* nervous system are associated with basal laminae (White et al., 1986), but, until recently, no matrix components had been localized to them. Antibody localizations of nidogen, NID-1 (Kang and Kramer, 2000), and CLE-1 (this report) to neural elements indicates that they are components of these neural basement membranes. Mutations in *nid-1* (Kim and Wadsworth, 2000; Kang and Kramer, 2000) and *cle-1* disrupt normal neural patterning, indicating that these matrix molecules have important roles in development of the *C. elegans* nervous system.

The *cg120* CLE-1 NC1 domain deletion results in multiple cell and axon migration defects, but very little (<5%) lethality. However, placing *cg120* across from a larger deletion of the region or RNAi against *cle-1* results in much greater levels of lethality (25–39%). The NC1 domain deletion is clearly only a partial loss-of-function mutation, and stronger loss-of-function appears to increase lethality. Although RNAi can generate apparent null phenotypes, some neuronally expressed genes have been shown to be refractory to RNAi (Tavernarakis et al., 2000). Since RNAi in the *cg120* background results in more penetrant lethality than in the wild-type background, it is likely that *cle-1* function is only partially inhibited by RNAi. Complete loss of *cle-1* function may result in more highly penetrant or strict lethality. The embryonic lethal animals from *cle-1* RNAi appear similar to mutants that disrupt epidermal (hypodermal) function (Williams-Masson et al., 1997; Costa et al., 1998), suggesting that CLE-1 may function in epidermal migration and/or adhesion.

In *C. elegans*, several lines of evidence indicate that cell migration and axon guidance require integration of a variety of signals (Wadsworth and Hedgecock, 1996). The migration defects we have described in *cg120* mutants are not fully penetrant, indicating that the CLE-1 NC1 domain is only one of the factors influencing these migrations. In fact, most mutations that affect cell and axon migrations in *C. elegans* are only partially penetrant (Wadsworth and Hedgecock, 1996). Mutations in two genes—*ina-1,* an α-integrin (Baum and Garriga, 1997), and *mig-2*, a Rac-like GTPase (Zipkin et al., 1997)—cause partially penetrant migration defects that are most similar to *cg120*. Interestingly, Kuo et al. (2001, this issue) demonstrate that the promigratory activity of the type XVIII collagen NC1 domain requires Rac and Cdc42 function. The relationship between *cle-1*, *ina-1*, and *mig-2* is currently being investigated.

We have shown that the CLE-1 NC1/ES domain affects cell and axon migrations in *C. elegans*. The collagen XVIII ES domain has antiangiogenic activity and has been reported to inhibit migration of endothelial cells specifically (O'Reilly et al., 1997; Dhanabal et al., 1999). Nematodes lack endothelial cells, but we have demonstrated effects on neurons and other cells. When cultured on complex matrix such as Matrigel, the migrations of other mammalian cell types, including neurons, were recently shown to respond to collagen XVIII NC1/ES domains (Kuo et al., 2001, this issue). In complex natural environments, the migrations of multiple cell types can be affected by mammalian and nematode collagen XVIII NC1/ES domains, indicating a conservation of function from nematodes to vertebrates.

In *cle-1(cg120)* NC1 domain deletion mutants, the migrations of multiple cells are incomplete, suggesting that the *C. elegans* NC1 domain has promigratory activity. Ectopic *cle-1* ES domain expression in the wild-type background causes similar cell migration defects, indicating that ES has antimigratory activity (Fig. 8 B). Ectopic ES does not exacerbate the migration defects caused by the NC1 deletion, suggesting that ES negatively regulates the NC1 promigratory activity. These findings are consistent with those of Kuo et al. (2001, this issue), showing that trimeric collagen XVIII NC1 or oligomerized ES domains have promigratory activity for several cell types and that monomeric ES inhibits these activities. The *C. elegans* NC1 and ES domains are, respectively, trimeric and monomeric in vitro, suggesting that differences in oligomerization may explain their different in vivo effects. Multivalency of ES domains could be important to cluster receptors or the matrix molecules to which they bind, as a means of activation (Giancotti and Ruoslahti, 1999).

The type XVIII collagen NC1/ES domain has a conserved role in regulating cell motility from *C. elegans* to vertebrates. In *C. elegans*, it most notably affects neurogenesis, presumably because this process involves numerous long range cell and axon migrations. In vertebrates, the best documented effects are on angiogenesis, which also involves extensive cell migrations. Related mechanisms may control cell migrations in neurogenesis and angiogenesis, and indeed molecules such as neuropilin (Soker et al., 1998) have been shown to affect migrations of both neural and endothelial cells. The role of type XVIII collagen in *C. elegans* neurogenesis suggests that it may also affect vertebrate neuronal cells.

We thank Y. Kohara (National Institute for Genetics, Mishima, Japan) for cDNA clones, A. Coulson (Sander Centre, London, UK) for cosmids, and A. Fire (Carnegie Institution of Washington, Baltimore, MD) for expression vectors. We thank J. Culotti (Samuel Lunenfeld Research Institute, Toronto, Ontario, Canada), C. Kenyon (University of California, San Francisco, CA), and D. Pilgrim (University of Alberta, Edmonton, Alberta, Canada) for GFP marker strains. We are indebted to K. Javaherian

and S. Park (Childrens Hospital, Harvard Medical School, Boston, MA) for purification and analysis of recombinant CLE-1 fragments. Some strains used in these studies were provided by the *Caenorhabditis elegans* Genetics Center, which is supported by the National Institutes of Health Center for Research Resources.

This work was supported by grants from the Health Sciences Council of the Academy of Finland (T. Pihlajaniemi) and the National Institutes of Health (HD27211, J.M. Kramer).

Submitted: 22 August 2000
Revised: 18 January 2001
Accepted: 19 January 2001

References

Barstead, R.J. 1999. Reverse genetics. *In C. elegans*: A Practical Approach. I.A. Hope, editor. Oxford University Press, Oxford, UK. 97–118.

Baum, P.D., and G. Garriga. 1997. Neuronal migrations and axon fasciculation are disrupted in *ina-1* integrin mutants. *Neuron*. 19:51–62.

Bettinger, J.C., K. Lee, and A.E. Rougvie. 1996. Stage-specific accumulation of the terminal differentiation factor LIN-29 during *Caenorhabditis elegans* development. *Development.* 122:2517–2527.

Boehm, T., J. Folkman, T. Browder, and M.S. O'Reilly. 1997. Antiangiogenic therapy of experimental cancer does not induce acquired drug resistance. *Nature.* 390:404–407.

Brenner, S. 1974. The genetics of *Caenorhabditis elegans*. *Genetics.* 77:71–94.

Burdine, R.D., E.B. Chen, S.F. Kwok, and M.J. Stern. 1997. *egl-17* encodes an invertebrate fibroblast growth factor family member required specifically for sex myoblast migration in *Caenorhabditis elegans*. *Proc. Natl. Acad. Sci. USA.* 94:2433–2437.

Chan, S. S., H. Zheng, M.W. Su, R. Wilk, M.T. Killeen, E.M. Hedgecock, and J.G. Culotti. 1996. UNC-40, a *C. elegans* homolog of DCC (deleted in colorectal cancer), is required in motile cells responding to UNC-6 netrin cues. *Cell.* 87:187–195.

Colavita, A., and J.G. Culotti. 1998. Suppressors of ectopic UNC-5 growth cone steering identify eight genes involved in axon guidance in *Caenorhabditis elegans*. *Dev. Biol*. 194:72–85.

Colavita, A., S. Krishna, H. Zheng, R.W. Padgett, and J.G. Culotti. 1998. Pioneer axon guidance by UNC-129, a *C. elegans* TGF-beta. *Science.* 281:706–709.

Costa M., W. Raich, C. Agbunag, B. Leung, J. Hardin, and J.R. Priess. 1998. A putative catenin–cadherin system mediates morphogenesis of the *Caenorhabditis elegans* embryo. *J. Cell Biol.* 141:297–308.

Culotti, J.G., and D.C. Merz. 1998. DCC and netrins. *Curr. Opin. Cell Biol.* 10: 609–613.

Desai, C., and H.R. Horvitz. 1989. *Caenorhabditis elegans* mutants defective in the functioning of the motor neurons responsible for egg laying. *Genetics.* 121:703–721.

Dhanabal, M., R. Ramchandran, M.J.F. Waterman, H. Lu, B. Knebelmann, M. Segal, and V.P. Sukhatme. 1999. Endostatin induces endothelial cell apoptosis. *J. Biol. Chem.* 274:11721–11726.

Dinbergs, I.D., L. Brown, and E.R. Edelman. 1996. Cellular response to transforming growth factor-beta1 and basic fibroblast growth factor depends on release kinetics and extracellular matrix interactions. *J. Biol. Chem.* 271: 29822–29829.

Emmons, S.W. 1992. From cell fates to morphology: developmental genetics of the *Caenorhabditis elegans* male tail. *BioEssays.* 14:309–316.

Fire, A., S.W. Harrison, and D. Dixon. 1990. A modular set of lacZ fusion vectors for studying gene expression in *Caenorhabditis elegans*. *Gene.* 93:189–198.

Fire, A., S. Xu, M.K. Montgomery, S.A. Kostas, S.E. Driver, and C.C. Mello. 1998. Potent and specific genetic interference by double-stranded RNA in *Caenorhabditis elegans*. *Nature.* 391:806–811.

Garriga, G., C. Desai, and H.R. Horvitz. 1993. Cell interactions control the direction of outgrowth, branching and fasciculation of the HSN axons of *Caenorhabditis elegans*. *Development.* 117:1071–1087.

Gettner, S.N., C. Kenyon, and L.F. Reichardt. 1995. Characterization of beta *pat-3* heterodimers, a family of essential integrin receptors in *C. elegans*. *J. Cell Biol.* 129:1127–1141.

Giancotti, F.G., and E. Ruoslahti. 1999. Integrin signaling. *Science.* 285:1028–1032.

Graham, P.L., J.J. Johnson, S.R. Wang, M.H. Sibley, M.C. Gupta, and J.M. Kramer. 1997. Type IV collagen is detectable in most, but not all, basement membranes of *Caenorhabditis elegans* and assembles on tissues that do not express it. *J. Cell Biol.* 137:1171–1183.

Guo, X.D., J.J. Johnson, and J.M. Kramer. 1991. Embryonic lethality caused by mutations in basement membrane collagen of *C. elegans*. *Nature.* 349:707–709.

Hagg, P.M., P.O. Hagg, S. Peltonen, H. AutioHarmainen, and T. Pihlajaniemi. 1997. Location of type XV collagen in human tissues and its accumulation in the interstitial matrix of the fibrotic kidney. *Am. J. Pathol.* 150:2075–2086.

Hamelin, M., Y. Zhou, M.W. Su, I.M. Scott, and J.G. Culotti. 1993. Expression of the UNC-5 guidance receptor in the touch neurons of *C. elegans* steers their axons dorsally. *Nature.* 364:327–330.

Hemler, M.E. 1999. Dystroglycan versatility. *Cell.* 97:543–546.

Hutter, H., B.E. Vogel, J.D. Plenefisch, C.R. Norris, R.B. Proenca, J. Spieth, C. Guo, S. Mastwal, X. Zhu, J. Scheel, and E.M. Hedgecock. 2000. Conservation and novelty in the evolution of cell adhesion and extracellular matrix genes. *Science.* 287:989–994.

Ishii, N., W.G. Wadsworth, B.D. Stern, J.G. Culotti, and E.M. Hedgecock. 1992. UNC-6, a laminin-related protein, guides cell and pioneer axon migrations in *C. elegans*. *Neuron.* 9:873–881.

Jones, J.L., and R.A. Walker. 1999. Integrins: a role as cell signaling molecules. *Mol. Pathol.* 52:208–213.

Kang, S.H., and J.M. Kramer. 2000. Nidogen is nonessential and not required for normal type IV collagen localization in *Caenorhabditis elegans*. *Mol. Cell. Biol*. 11:3911–3923.

Kim, S., and W.G. Wadsworth. 2000. Positioning of longitudinal nerves in *C. elegans* by nidogen. *Science* 288:150–154.

Kivirikko, S., P. Heinamaki, M. Rehn, N. Honkanen, J.C. Myers, and T. Pihlajaniemi. 1994. Primary structure of the alpha 1 chain of human type XV collagen and exon-intron organization in the 3′ region of the corresponding gene. *J. Biol. Chem.* 269:4773–4779.

Kramer, J.M. 1997. Extracellular matrix structure and function. *In* The Nematode *C. elegans*. Vol. 2. D.L. Riddle, editor. Cold Spring Harbor Laboratory Press, Cold Spring Harbor, NY. 471–500.

Kuo, C.J., K.R. LaMontagne, Jr., G. Garcia-Cardeña, B.D. Ackley, D. Kalman, S. Park, R. Christofferson, J. Kamihara, Y.-H. Ding, K.-M. Lo, et al. 2001. Oligomerization-dependent regulation of motility and morphogenesis by the collagen XVIII NC1/endostatin domain. *J. Cell Biol.* 152:1233–1246.

Mello, C.C., J.M. Kramer, D. Stinchcomb, and V. Ambros. 1991. Efficient gene transfer in *C. elegans*: extrachromosomal maintenance and integration of transforming sequences. *EMBO (Eur. Mol. Biol. Organ.) J.* 10:3959–3970.

Muragaki, Y., N. Abe, Y. Ninomiya, B.R. Olsen, and A. Ooshima. 1994. The human alpha 1(XV) collagen chain contains a large amino-terminal non-triple helical domain with a tandem repeat structure and homology to alpha 1(XVIII) collagen. *J. Biol. Chem.* 269:4042–4046.

Muragaki, Y., S. Timmons, C.M. Griffith, S.P. Oh, B. Fadel, T. Quertermous, and B.R. Olsen. 1995. Mouse Col18a1 is expressed in a tissue-specific manner as three alternative variants and is localized in basement membrane zones. *Proc. Natl. Acad. Sci. USA.* 92:8763–87677.

Musso, O., M. Rehn, J. Saarela, N. Theret, J. Lietard, L.D. Hintikka, J.P. Campion, T. Pihlajaniemi, and B. Clement. 1998. Collagen XVIII is localized in sinusoids and basement membrane zones and expressed by hepatocytes and activated stellate cells in fibrotic human liver. *Hepatology.* 28:98–107.

Oh, S.P., Y. Kamagata, Y. Muragaki, S. Timmons, A. Ooshima, and B.R. Olsen. 1994a. Isolation and sequencing of cDNAs for proteins with multiple domains of Gly-Xaa-Yaa repeats identify a distinct family of collagenous proteins. *Proc. Natl. Acad. Sci. USA.* 91:4229–4233.

Oh, S.P., M.L. Warman, M.F. Seldin, S.D. Cheng, J.H. Knoll, S. Timmons, and B.R. Olsen. 1994b. Cloning of cDNA and genomic DNA encoding human type XVIII collagen and localization of the alpha 1(XVIII) collagen gene to mouse chromosome 10 and human chromosome 21. *Genomics.* 19:494–499.

O'Reilly, M.S., T. Boehm, Y. Shing, N. Fukai, G. Vasios, W.S. Lane, E. Flynn, J.R. Birkhead, B.R. Olsen, and J. Folkman. 1997. Endostatin: an endogenous inhibitor of angiogenesis and tumor growth. *Cell.* 88:277–285.

Ramchandran, R., M. Dhanabal, R. Volk, M.J. Waterman, M. Segal, H. Lu, B. Knebelmann, and V.P. Sukhatme. 1999. Antiangiogenic activity of restin, NC10 domain of human collagen XV: comparison to endostatin. *Biochem. Biophys. Res. Commun.* 255:735–739.

Rehn, M., and T. Pihlajaniemi. 1994. Alpha 1(XVIII), a collagen chain with frequent interruptions in the collagenous sequence, a distinct tissue distribution, and homology with type XV collagen. *Proc. Natl. Acad. Sci. USA.* 91: 4234–4238.

Rehn, M., and T. Pihlajaniemi. 1995. Identification of three N-terminal ends of type XVIII collagen chains and tissue-specific differences in the expression of the corresponding transcripts. The longest form contains a novel motif homologous to rat and *Drosophila* frizzled proteins. *J. Biol. Chem.* 270:4705–4711.

Rehn, M., E. Hintikka, and T. Pihlajaniemi. 1994. Primary structure of the alpha 1 chain of mouse type XVIII collagen, partial structure of the corresponding gene, and comparison of the alpha 1(XVIII) chain with its homologue, the alpha 1(XV) collagen chain. *J. Biol. Chem.* 269:13929–13935.

Rogalski, T.M., B.D. Williams, G.P. Mullen, and D.G. Moerman. 1993. Products of the *unc-52* gene in *Caenorhabditis elegans* are homologous to the core protein of the mammalian basement membrane heparan sulfate proteoglycan. *Genes Dev*. 7:1471–1484.

Saarela, J., M. Rehn, A. Oikarinen, H. Autio-Harmainen, and T. Pihlajaniemi. 1998a. The short and long forms of type XVIII collagen show clear tissue specificities in their expression and location in basement membrane zones in humans. *Am. J. Pathol.* 153:611–626.

Saarela, J., R. Ylikarppa, M. Rehn, S. Purmonen, and T. Pihlajaniemi. 1998b. Complete primary structure of two variant forms of human type XVIII collagen and tissue-specific differences in the expression of the corresponding transcripts. *Matrix Biol.* 16:319–328.

Sasaki, T., N. Fukai, K. Mann, W. Göhring, B.R. Olsen, and R. Timpl. 1998. Structure, function and tissue forms of the C-terminal globular domain of

collagen XVIII containing the angiogenesis inhibitor endostatin. *EMBO (Eur. Mol. Biol. Organ.) J.* 17:4249–4256.

Sasaki, T., H. Larsson, D. Tisi, L. Claesson-Welsh, E. Hohenester, and R. Timpl. 2000. Endostatins derived from collagens XV and XVIII differ in structural and binding properties, tissue distribution and anti-angiogenic activity. *J. Mol. Biol.* 301:1179–1190.

Sibley, M.H., P.L. Graham, N. von Mende, and J.M. Kramer. 1994. Mutations in the α2(IV) basement membrane collagen gene of *Caenorhabditis elegans* produce phenotypes of differing severities. *EMBO (Eur. Mol. Biol. Organ.) J.* 13:3278–3285.

Soker, S., S. Takashima, H.Q. Miao, G. Neufeld, and M. Klagsbrun. 1998. Neuropilin-1 is expressed by endothelial and tumor cells as an isoform-specific receptor for vascular endothelial growth factor. *Cell.* 92:735–745.

Stringa, E., V. Knauper, G. Murphy, and J. Gavrilovic. 2000. Collagen degradation and platelet-derived growth factor stimulate the migration of vascular smooth muscle cells. *J. Cell Sci.* 113:2055–2064.

Sulston, J.E., D.G. Albertson, and J.N. Thomson. 1980. The *Caenorhabditis elegans* male: postembryonic development of nongonadal structures. *Dev. Biol.* 78:542–576.

Sze, J.Y., M. Victor, C. Loer, Y. Shi, and G. Ruvkun. 2000. Food and metabolic signalling defects in a *Caenorhabditis elegans* serotonin-synthesis mutant. *Nature.* 403:560–564.

Tavernarakis, N., S.L. Wang, M. Dorovkov, A. Ryazanov, and M. Driscoll. 2000. Heritable and inducible genetic interference by double-stranded RNA encoded by transgenes. *Nat. Genet.* 24:180–183.

Vogel, W. 1999. Discoidin domain receptors: structural relations and functional implications. *FASEB J.* 13:S77–S82.

Wadsworth, W.G., and E.M. Hedgecock. 1996. Hierarchical guidance cues in the developing nervous system of *C. elegans*. *Bioessays.* 18:355–362.

White, J.G., E. Southgate, J.N. Thomson, and S. Brenner. 1986. The structure of the nervous system of *Caenorhabditis elegans*. *Philos. Trans. R. Soc. Lond. Ser. B Biol. Sci.* 314:1–340.

Williams, B.D., and R.H. Waterston. 1994. Genes critical for muscle development and function in *Caenorhabditis elegans* identified through lethal mutations. *J. Cell Biol.* 124:475–490.

Williams-Masson, E.M., A.N. Malik, and J. Hardin. 1997. An actin-mediated two-step mechanism is required for ventral enclosure of the *C. elegans* hypodermis. *Development.* 24:2889–2901.

Yamaguchi, N., B. Anand-Apte, M. Lee, T. Sasaki, N. Fukai, R. Shapiro, I. Que, C. Lowik, R. Timpl, and B.R. Olsen. 1999. Endostatin inhibits VEGF-induced endothelial cell migration and tumor growth independently of zinc binding. *EMBO (Eur. Mol. Biol. Organ.) J.* 18:4414–4423.

Zipkin, I.D., R.M. Kindt, and C.J. Kenyon. 1997. Role of a new Rho family member in cell migration and axon guidance in *C. elegans*. *Cell.* 90:883–894.